Percolation-Limited Ionic Diffusion in $Li_{0.5-x}Na_xLa_{0.5}TiO_3$ Perovskites ($0 \leq x \leq 0.5$)

A. Rivera,[†,‡] C. León,[†] J. Santamaría,[†] A. Várez,[§] O. V'yunov,[∥] A. G. Belous,[∥] J. A. Alonso,[‡] and J. Sanz*[,‡]

GFMC, Departamento Física Aplicada III, Universidad Complutense Madrid, 28040 Madrid, Spain, Instituto Ciencia de Materiales de Madrid-CSIC, Cantoblanco, 28049 Madrid, Spain, Departamento Ciencia de Materiales, Universidad Carlos III de Madrid, 28911 Leganés, Spain, and Solid State Chemistry, Institute of Inorganic Chemistry, Ukrainian Academy of Sciences, 252680, Ukraine

Received July 24, 2002. Revised Manuscript Received September 9, 2002

The dependence of ionic transport properties on the structure and composition of perovskites $Li_{0.5-x}Na_xLa_{0.5}TiO_3$ ($0 \leq x \leq 0.5$) has been analyzed by means of ND, XRD, NMR, and impedance spectroscopy. Local lithium mobility is shown to decrease progressively by 2 orders of magnitude along the series; however, long-range dc conductivity decreases sharply at $x = 0.2$ more than 6 orders of magnitude. The decrease of dc conductivity from values typical of fast ionic conductors, 10^{-3} S/cm at room temperature, to values of insulators, 10^{-10} S/cm, is discussed in terms of a three-dimensional percolation model for lithium diffusion. As deduced from XRD and ND data, the number of vacant sites in conduction pathways is controlled by the amount of Na and La in the perovskite.

Introduction

Interest in ionic-conducting solids has been increasing in the past years because of their potential application as solid electrolytes in batteries, fuel cells, and other devices.[1,2] Ionic conductivity is favored by a disordered distribution of mobile ions in structures containing vacant sites that are energetically equivalent (or nearly equivalent) to sites occupied by the mobile ions. The presence of vacant sites allows the ions to hop from site to site through the structure and eventually gives rise to a long-range or dc ionic transport. Ionic conductivity is thus proportional to the concentration of mobile ions, n_c, and to their mobility, which increases with the amount of vacant sites n_v. Therefore, one of the strategies commonly used in the search for novel ionically conducting materials consists of the optimization of the product $n_c n_v$ by the partial substitution of certain ions by others with different valences in structures with open conduction pathways.

In the case of the fast ionic conductors $Li_yLa_{(2-y)/3}\square_{(1-2y)/3}TiO_3$, $0 < y < 0.5$ (LLTO series), La^{3+} ions in A sites of the perovskite (ABO_3) can be substituted by Li^+ ions, and the number of nominal vacant A sites is given by $\square = (1 - 2y)/3$. Since the discovery of outstanding electrical properties of these materials,[3,4] several groups have investigated the role played by the vacant A sites in the ionic conductivity of these materials.[5−12] For a random distribution of vacant sites, a maximum conductivity would be expected for a lithium content of $y = 0.25$ (maximum $n_c n_v$ product), while it should vanish at $y = 0$ and $y = 0.5$. However, the highest value of dc conductivity ($\sigma_{dc} \sim 10^{-3}$ S/cm at room temperature) is found for a lithium content $y = 0.31$, and unexpectedly high dc conductivity values have been reported for samples with y close to 0.5.[11] Inaguma and Itoh[12] proposed the existence of a percolation-limited motion of lithium ions as the reason for the shift observed in the maximum of the dc conductivity to higher lithium contents. On the other hand, a recent neutron diffraction study of a sample with $y = 0.5$ has provided an explanation for the high dc conductivity values measured in Li-rich perovskites. It was observed that lithium ions are not located at A sites but distributed at unit-cell faces of the perovskite.[13] In this case, the amount of vacant A sites would be considerably higher than that deduced from the structural formula.

* To whom correspondence should be addressed.
[†] Universidad Complutense Madrid.
[‡] Instituto Ciencia de Materiales de Madrid-CSIC.
[§] Universidad Carlos III de Madrid.
[∥] Ukrainian Academy of Sciences.

(1) Colbow, K. M.; Dahn, J. R.; Hearing, R. R. *J. Power Sources* **1989**, *26*, 397.
(2) Robertson, A. D.; West, A. R.; Ritchie A. G. *Solid State Ionics* **1997**, *104*, 1.
(3) Belous, A. G.; Novitskaya, G. N.; Polyanetskaya, S. V.; Gornikov, Yu. I. *Izv. Akad. Nauk SSSR, Neorg. Mater.* **1987**, *23*, 470.
(4) Inaguma, Y.; Liquan, C.; Itoh, M.; Nakamura, T.; Uchida, T.; Ikuta, H.; Wakihara, M. *Solid State Commun.* **1993**, *86*, 689.
(5) Itoh, M.; Inaguma, Y.; Jung, W. H.; Chen, L.; Nakamura, T. *Solid State Ionics* **1994**, *70−71*, 203.
(6) Kawai, H.; Kuwano, J. *J. Electrochem Soc.* **1994**, *147*, L78−79.
(7) Robertson, A. D.; García-Martín, S.; Coats, A.; West, A. R. *J. Mater. Chem.* **1995**, *5*, 1405.
(8) Bohnke, O.; Bohnke, C.; Ould Sid'Ahmed, J.; Crosnier-Lopez, M. P.; Duroy, H.; Le Berre, F.; Fourquet, J. L. *Chem. Mater.* **2001**, *13*, 1593.
(9) Harada, Y.; Hirakoso, Y.; Kawai, H.; Kuwano, J. *Solid State Ionics* **1999**, *121*, 245.
(10) París, M. A.; Sanz, J.; León, C.; Santamaría, J.; Ibarra, J.; Várez, A.; *Chem. Mater.* **2000**, *12*, 1694.
(11) Ibarra, J.; Várez, A.; León, C.; Santamaría, J.; Torres-Martínez, L. M.; Sanz, J. *Solid State Ionics* **2000**, *134*, 219.
(12) Inaguma, Y.; Itoh, M. *Solid State Ionics* **1996**, *86−88*, 257.
(13) Alonso, J. A.; Sanz, J.; Santamaría, J.; León, C.; Várez, A.; Fernández-Díaz, M. T. *Angew. Chem., Int. Ed.* **2000**, *39*, 619.

10.1021/cm0204627 CCC: $22.00
Published on Web 11/13/2002

This fact on its own can also explain the shift to higher lithium contents of the highest dc conductivity value. Nevertheless, a percolation-limited ionic motion has not been discarded, and the composition dependence of the ionic conductivity in LLTO series remains an open question.

On the other hand, it has been recently reported that the analogue sample with sodium instead of lithium, $Na_{0.5}La_{0.5}TiO_3$, is not an ionic conductor but behaves like an insulator.[14,15] The higher size of sodium compared to that of lithium justifies a better coordination of sodium ions at A sites. The very different electrical properties of the end members of the solid solution $Li_{0.5-x}Na_xLa_{0.5}TiO_3$ (LNLTO), with $0 \leq x \leq 0.5$, has motivated the investigation of structure and transport properties of this series. Structural features of this series have been deduced from the Rietveld analysis of neutron diffraction patterns. ^{7}Li and ^{23}Na NMR spectroscopies have been used to analyze the local mobility of alkali ions and dc conductivity data obtained by impedance spectroscopy to determine the long-range ionic transport. A sharp decrease is observed in the dc conductivity when the sodium content increases above $x = 0.2$, while the unit cell parameters of the structure remain essentially unchanged. This behavior is interpreted in terms of a three-dimensional percolation-limited diffusion of lithium ions through vacant A sites of the perovskite.

Experimental Section

Samples of the series $Li_{0.5-x}Na_xLa_{0.5}TiO_3$ (with $x = 0$, 0.1, 0.15, 0.18, 0.2, 0.3, 0.4, and 0.5) were synthesized from the stoichiometric amount of Li_2CO_3, Na_2CO_3, La_2O_3, and TiO_2 (high-purity grade). Li_2CO_3 and Na_2CO_3 compounds were dried at 300 °C, La_2O_3 at 800 °C, and TiO_2 at 600 °C. The mixtures were ground and calcined in air for 4 h at 1050 °C. To avoid the loss of alkaline elements, the temperature was increased slowly (1 °C/min). The calcined powders were ground, pressed into pellets under a pressure of 500 kg/cm^2 (50 MPa), and finally sintered at 1300 °C.

Samples were first characterized by X-ray diffraction. Powder patterns were recorded with Cu Kα radiation in a X'Pert Phillips diffractometer, with ($\theta/2\theta$) Bragg-Bentano geometry, equipped with a curved graphite monochromator. Data were taken with a 0.5° divergence slit and a receiving slit of 0.01°. The 2θ range analyzed was 10−90°, with a step scan of 0.02° and a counting time of 10 s. XRD patterns were indexed with the Treor program.

ND patterns of samples with $x = 0$, 0.2, and 0.5 were recorded at 295 K in D2B ($\lambda = 1.954$ Å) and D1A ($\lambda = 1.913$ Å) diffractometers of ILL-Grenoble. To reduce the absorption section of samples, ^{7}Li-enriched perovskites were prepared. ND patterns of powder samples (4 g) were collected between 5 and 160° 2θ with a step scan of 0.02° (4 h). For the Rietveld analysis of ND profiles (Fullprof program) a pseudo-Voigt function was chosen to describe the line shape of diffraction peaks. The coherent scattering lengths for La, Li, Na, Ti, and O atoms were respectively 8.24, −1.90, 3.63, −3.30, and 5.80 fm.

^{7}Li and ^{23}Na NMR spectra were obtained at room temperature in a MSL-400 Bruker spectrometer working at 155.45 and 104.8 MHz. Static and magic angle spinning (MAS) NMR spectra were taken after irradiation of the sample with a $\pi/2$ pulse (3 μs). In MAS experiments, the rotor used was of the Andrew type with a spinning frequency of 4 kHz. Determination of T_1 spin lattice relaxation (SLR) times at room temperature was done by using the $\pi-\tau-\pi/2$ sequence for ^{7}Li and the $\pi/2-\tau-\pi/2$ sequence for ^{23}Na NMR signals. Analysis of NMR spectra was carried out with the Winfit software (Bruker). This program allows the position, line width, and intensity of the components to be determined by using a nonlinear least-squares method. However, quadrupole constants C_Q and η must be determined by a trial and error procedure.

Sintered cylindrical pellets 16 mm in diameter and 1-mm thick, with silver electrodes on both faces, were used for electrical measurements. Impedance spectroscopy was conducted in the frequency range 20 Hz to 30 MHz at temperatures between 180 and 516 K, using precision LCR meters HP4284A and HP4285A. Measurements were carried out under a N_2 flow to ensure an inert atmosphere.

Table 1. Structural Information Deduced from Refinement of ND Patterns of $Li_{0.5-x}Na_xLa_{0.5}TiO_3$ Samples[a]

	$x = 0$	$x = 0.2$	$x = 0.5$
a (Å)	5.4712(3)	5,4799(1)	5.4868(1)
c (Å)	13,4046(7)	13,4230(7)	13,4239(5)
V (Å^3)	347.49(3)	349.08 (2)	349.99(2)
R_p	5.18	5.86	5.29
R_{wp}	7.23	7.89	7.19
R_B	3.93	3.62	2.88
R_F	3.75	2.98	2,55
X^2	7.67	3.36	2,66
La occ	0.504(10)	0.498(10)	0.501(11)
B_{iso}	0.10(3)	0.25(6)	0.68(7)
3*Li occ	0.495(40)	0.210(30)	
B_{iso}	10.1(9)	9.2 (9)	
Na occ		0.177(20)	0.480(20)
B^{iso}		0.25(6)	0.68(8)
Ti B_{iso}	1.08(12)	0.51(7)	0.48(7)
O x	0.5317(5)	0.5397(3)	0.5396(3)
B_{iso}	1.75(8)	1.29(9)	1.02(8)
Ti−O	1.942(2)	1.949(2)	1.951(2)
$(M-O)_{av.}$	2.739(2)	2.744(1)	2.744(2)
$(Li-O)_{av.}$	1.938(9)	1.943(8)	
$(O-O)_{l.}$	4.121(5)	4.190(5)	4.192(5)
$(O-O)_{s.}$	3.632(5)	3.584(5)	3.588(5)
Ti−O−Ti	169.8(4)	167.3(3)	167.4(4)

[a] Thermal factors of La and Na cations were constrained to vary together during refinement

Results

XRD and ND patterns of $Li_{0.5-x}Na_xLa_{0.5}TiO_3$ samples show in all cases the presence of a single phase, displaying a rhombohedral $R\bar{3}c$ symmetry, with unit cell parameters near $a = 5.48$ Å and $c = 13.42$ Å (see Table 1). Cubic (a_p,a_p,a_p) and orthorhombic ($\sqrt{2}a_p$,$\sqrt{2}a_p$,$2a_p$) perovskite unit cells were discarded; the cubic model did not account for small XRD superstructure peaks, while the orthorhombic cell displayed a much higher number of reflections than those observed in XRD patterns. Similar conclusions were deduced from the analysis of ND patterns, where superstucture peaks of the rhombohedral phase are clearly visible (arrows of Figure 1).

Structural features of LNLTO have been deduced from the Rietveld analysis of XRD and ND patterns. In both cases, the experimental parameters, scale factor, background coefficients, 2θ zero position, halfwidth, and peak-shape parameters, were first determined. In XRD analysis, microabsorption processes produced negative thermal factors. However, in ND analysis, positional

(14) Rao, R. M. V.; Munekata, H.; Shimada, K.; Lippmaa, M.; Kawasaki, M.; Inaguma, Y.; Itoh, M.; Koinuma, H. *J. Appl. Phys.* **2000**, *88*, 3756.

(15) Belous, A. G. *Third Euro-Ceram.* **1993**, *2*, 341.

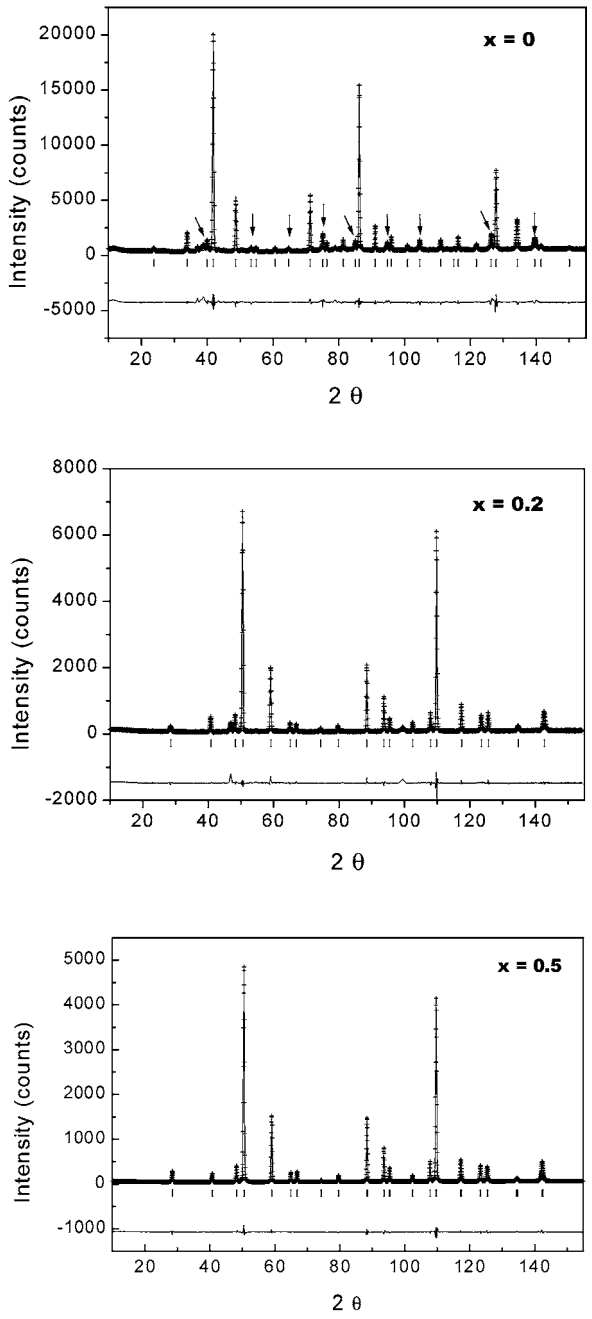

Figure 1. Rietveld refinement of ND patterns of $Li_{0.5-x}Na_xLa_{0.5}TiO_3$ samples, with $x = 0$, 0.2, and 0.5, assuming the $R\bar{3}c$ space group. ND pattern of $x = 0$ was recorded with $\lambda = 1.594$ Å and those of $x = 0.2$ and 0.5 with $\lambda = 1.913$ Å. Superstructure peaks associated with the rhombohedral symmetry are indicated with arrows. The solid line is a fit of calculated to experimental data (crosses). Difference between measured and calculated intensities is given at the bottom. Bars correspond to Bragg peak positions.

parameters, atomic occupations, and isotropic/anisotropic factors for Li, Na, La, Ti and O atoms were all reasonable (see Table 1). Agreement R_B factors were lower than 4% and R_{WP} factors lower than 8% for all samples. The fitting of ND patterns of samples with $x = 0$, 0.2, and 0.5 are shown in Figure 1.

Structural analysis showed that Na and La ions are located at A sites of the perovskite. However, as previously shown in a recent work, Li ions occupy the center of unit cell faces of the ideal perovskite.[13] In all cases, occupations deduced for A sites agree with nominal

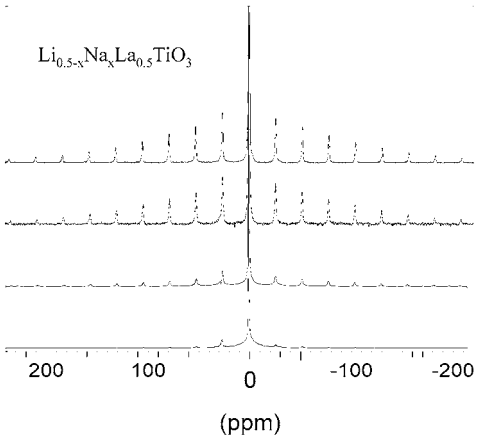

Figure 2. ^{7}Li MAS NMR spectra of $Li_{0.5-x}Na_xLa_{0.5}TiO_3$ series. Equally spaced sidebands are produced by the spinning of the sample around the magic angle. Lithium contents are 0.1, 0.2, 0.3, and 0.4, from the top to the bottom.

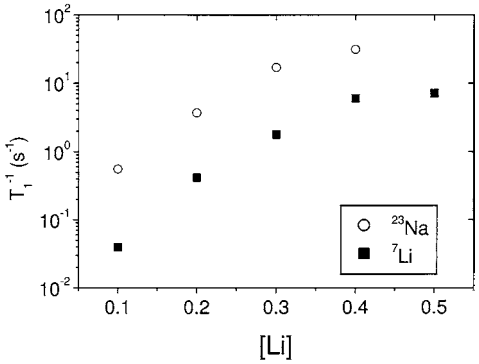

Figure 3. ^{7}Li and ^{23}Na SLR rates versus the lithium content of $Li_{0.5-x}Na_xLa_{0.5}TiO_3$ series.

compositions. Isotropic thermal factors of Li are considerably higher than those of Na, Ti, and La ions, indicating a higher mobility for Li^+ ions at room temperature.

Both ^{7}Li and ^{23}Na atoms have a nuclear spin $I = {}^3/_2$, and NMR spectra are formed by a central ($-{}^1/_2$, ${}^1/_2$) and two satellite (${}^1/_2$, ${}^3/_2$) and ($-{}^1/_2$, $-{}^3/_2$) transitions. In ^{7}Li MAS NMR spectra of LNLTO perovskites shown in Figure 2, these transitions are modulated by equally spaced bands associated with the sample spinning. The central line of ^{7}Li MAS NMR spectra is more intense than the one corresponding to the observed satellite transitions, indicating the presence of two lithium species with different mobility. The NMR spectrum of mobile species is formed by a single line with a quadrupole constant C_Q near zero. The NMR spectrum of less mobile species displays satellite transitions that are fitted in all samples with similar quadrupole parameters ($C_Q = 60$ kHz, $\eta = 0.5$). In Li-rich samples, the amount of mobile Li ions is maximum and the intensity of satellite transitions is minimum. As the sodium content increases, intensity of transitions associated with localized species increases. In the case of Na-rich samples, the amount of mobile Li species becomes very low (see Figure 2).

In Figure 3 we have plotted ^{7}Li and ^{23}Na relaxation (SLR) T_1^{-1} rates, deduced from the central transition of spectra at room temperature, as a function of the lithium content of perovskites. A single-exponential relaxation was detected in both signals. T_1^{-1} values

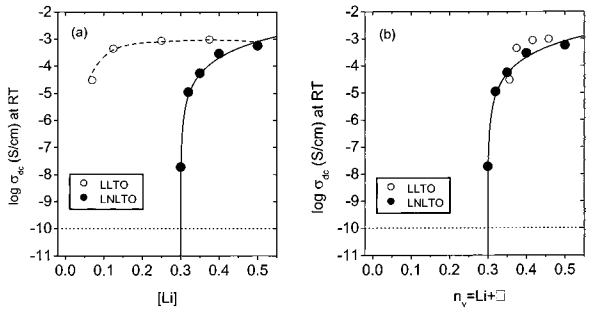

Figure 4. (a) Room-temperature dc conductivity of $Li_{0.5-x}Na_xLa_{0.5}TiO_3$ versus lithium content of the samples (solid circles). The continuous line is a fit of dc conductivity data to the expression $\sigma_{dc} = K(n - n_p)^2$, deduced for a percolation-limited diffusion of lithium ions in perovskites. A value of the percolation threshold $n_p = 0.30 \pm 0.01$ is obtained, in good agreement with that expected from the percolation model in a cubic lattice ($n_p \approx 0.31$). RT dc conductivity values are $<10^{-10}$ S/cm (our experimental resolution) for samples with $n < 0.3$. Room-temperature dc conductivity of $Li_yLa_{(2-y)/3}TiO_3$ samples are also plotted as a function of lithium content ($n = y$) for comparison (open circles). (b) Same data as in (a) but plotted versus the number $n_v = [Li] + \square$ of vacant A sites per formula unit (see text).

increase with the Li content, approaching a saturation value at [Li] = 0.4. In these perovskites, spin lattice relaxation is produced by fluctuations of quadrupolar interactions of nuclei with the electric field gradient at occupied sites.[10,16,17] This interaction is described by the quadrupole C_Q constant, given by the expression e^2QV_{zz}/h, where e is the electron charge, Q the quadrupole moment of nuclei, V_{zz} the principal value of the electric field gradient, and h Planck's constant. According to the higher quadrupolar moment of sodium, T_1^{-1} values deduced from the ^{23}Na signal are systematically higher than those deduced from the ^7Li signal. In both cases, T_1^{-1} values vary in the same way as the amount of the lithium mobile species.

Figure 4a shows the dependence of the dc conductivity at room temperature on the lithium content for the solid solution $Li_{0.5-x}Na_xLa_{0.5}TiO_3$ (solid circles). In the same figure, dc conductivity values of LLTO samples (open circles) have been included for comparison. LNLTO samples with low sodium contents ($x < 0.2$) display values of the dc conductivity in the range of 10^{-3} S/cm at 300 K, similar to those found in LLTO perovskites. The striking result is the sharp decrease observed in the dc conductivity down to 10^{-8} S/cm at room temperature for the sample with $x = 0.2$. When the sodium content is further increased, dc conductivity at RT is found to be $<10^{-10}$ S/cm, our experimental resolution limit.

Discussion

All samples analyzed display a rhombohedral $R\bar{3}c$ symmetry, with unit cell parameters that do not change appreciably with the composition. The structure of these perovskites is constituted by an octahedral network of regular polyhedra (Ti−O ∼ 1.94 Å) in which La cations are 12-fold coordinated. The octahedral tilting ($a^-a^-a^-$ in Glazer's notation) produced Ti−O−Ti angles near 167° and an oblique distortion of square windows that connect contiguous A sites of the perovskite. In these windows, diagonal O−O distances are near 3.60 and 4.20 Å (see Table 1), values that do not allow Na ions to pass through these windows and to contribute to the long-range ionic conduction. In accordance with this fact, the analysis of ND patterns showed that Na and La ions occupy A sites of the perovskite.

The Rietveld analysis of ND patterns of samples $Li_{0.5-x}Na_xLa_{0.5}TiO_3$ with $x < 0.2$ showed that Li ions are located at square windows (unit cell faces) that connect contiguous A sites of the perovskite. Average Li−O distances at these sites are near those corresponding to a 4-fold coordination of Li ions (2.0 Å). On the other hand, thermal factors deduced for Li are considerably higher than those deduced for Na, indicating that the mobility of Li ions is much more important than that of Na^+ ions. Some residual mobility is detected in octahedra, as deduced from the increase of O and Ti thermal factors, when the lithium content increases in perovskites (see Table 1). From this fact, diffusion of lithium through square windows is enhanced in Li-rich LNLTO samples.

The analysis of T_1^{-1} relaxation rates of Li^+ ions showed that the residence time of lithium at square windows is near 10^{-8} s at room temperature in $Li_{0.5}La_{0.5}TiO_3$.[16,17] As a consequence of the significant mobility of lithium, quadrupole interactions were averaged out ($C_Q \sim 0$ kHz) in ^7Li NMR spectra of this perovskite.[11] As the Na content increases in LNLTO samples, the amount of mobile Li species decreases and ^7Li NMR spectra display quadrupole satellite transitions of less mobile species (Figure 2). The intensity of satellite transitions increases with the sodium content; however, quadrupole parameters ($C_Q \sim 60$ kHz, $\eta = 0.5$) do not change with the composition. This fact suggests that structural sites occupied by lithium are the same and only the amount of mobile Li^+ ions change along the series. According to this observation, the decrease observed in T_1^{-1} relaxation rates will be due to a progressive decrease of the mean Li mobility. As far as sodium ions are concerned, their larger size precludes them from passing through the square windows. On the basis of this fact, changes observed on T_1^{-1} values of the ^{23}Na signal, similar to those detected in the ^7Li signal, have been ascribed to the relaxation induced by mobile Li ions at sites occupied by sodium cations. When all Li is moving, relaxation rates of two signals attain a saturation value.

If all A sites were occupied by alkaline cations, dc conductivity values of LNLTO samples will be near zero. However, measured values are very high in samples with $x < 0.2$, suggesting that part of the A sites might not be occupied. This hypothesis was confirmed by the Rietveld analysis of ND patterns, which showed that Li ions are located at the faces of the unit cells of perovskites. The amount of vacant A sites is then considerably higher than that deduced from the structural formula and this could explain the high values of dc conductivity measured in Li-rich perovskites. On the other hand, LNLTO samples with low lithium contents ($x > 0.2$) display a much lower dc conductivity than those obtained in the LLTO series (see Figure 4a). At

(16) León, C.; Lucía, M. L.; Santamaría, J.; París, M. A.; Sanz, J.; Várez, A. *Phys. Rev. B* **1996**, *54*, 184.
(17) León, C.; Santamaría, J.; París, M. A.; Sanz, J.; Ibarra, J.; Torres, L. M. *Phys. Rev. B* **1997**, *56*, 5302.

this point, it is important to remark that, in LNLTO samples, the amount of vacant A sites is considerably reduced when sodium increases.

To explain the steep decrease of the dc conductivity observed in LNLTO samples (Figure 4a), we have considered a percolation model for the lithium diffusion. In this model, A sites associated with Li ions are vacant and participate in ionic diffusion, but A sites occupied by La or Na ions do not participate in ionic conduction and block lithium diffusion. We expect ionic transport to give rise to a dc conductivity only for concentrations of vacant A sites above the percolation threshold, $n_p \approx 0.31$, and a composition dependence of the dc conductivity of the form $\sigma_{dc}=K(n - n_p)^2$, corresponding to the three-dimensional percolation of Li motion in the cubic network formed by A sites.[18,19] Interestingly, good agreement is found between the dc-conductivity values and those expected from the percolation model (see solid line of the Figure 4a). dc conductivity is very high when the number of vacant A sites per unit cell is higher than 0.3 ($x < 0.2$). At $x = 0.2$, the amount of vacancies is very close to the percolation threshold, and the infinite percolation cluster is about to disappear, reducing drastically the value of the dc conductivity.[18,19] For higher sodium contents, $x > 0.2$, all clusters are expected to be of finite size, and long-range ionic transport does not occur. The existence of percolation-limited lithium diffusion in LLTO perovskites was previously suggested to explain the lithium concentration dependence of the dc conductivity.[12] However, compositions analyzed in that work did not allow observation of its main feature, that is, a sharp decrease of several orders of magnitude in the dc conductivity, so it must be concluded that the percolation threshold was not reached in those samples.

In LNLTO samples, the presence of a percolation process for lithium diffusion does not contradict NMR SLR results obtained in this series. A decrease of local lithium mobility is observed when the sodium content is increased, due to a higher probability of finding neighboring A sites occupied (Figure 3); however, some mobility of Li ions can be preserved within finite clusters, even below the percolation threshold. This idea is illustrated in Figure 5, where a two-dimensional square lattice is shown with concentrations of vacant sites above, at, and below the percolation threshold. In Li-rich samples, a long-range mobility is favored; however, in Na-rich samples, only the local mobility of Li is possible (white arrows of Figure 5).

Our results suggest that the amount of vacancies available for lithium diffusion is defined by the sum of nominal vacancies plus the Li content,[13] $n_v = [Li] + \square$, and it is n_v which rules the percolation threshold. This is analyzed in Figure 4b, where we have plotted room-temperature dc-conductivity data for both the LLTO and

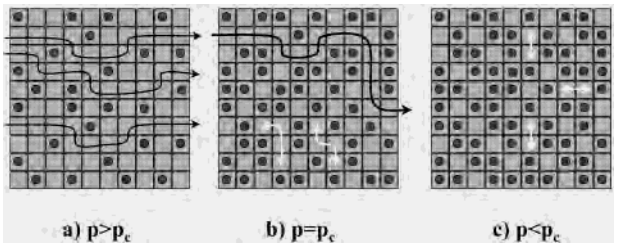

Figure 5. Schematic illustration of the percolation-limited motion above (a), at (b), and below (c) the percolation threshold for a two-dimensional square lattice. White arrows illustrate local mobility of Li in finite clusters.

LNLTO series as a function of n_v. In this plot, all points are placed in the curve deduced for a three-dimensional percolation of vacant A sites. From this fact, the amount of vacancies in $Li_yLa_{(2-y)/3}\square_{(1-2y)/3}TiO_3$ (LLTO) increases with the Li content from 0.33 to 0.5, values that are always above the percolation threshold ($n_v = 0.31$). The decrease of 2 orders of magnitude detected in dc conductivity of Li-poor LLTO perovskites, much larger than that expected for a dc-conductivity linearly dependent on the lithium content, shows the proximity of the percolation threshold in Li-poor samples (see Figure 4b). The composition dependence of the dc conductivity in LNLTO samples shows clearly the existence of a percolation process. Since Na ions are located at A sites of perovskites, they block the pathways for lithium diffusion. From this fact, the number $n_v = [Li] + \square$ becomes the most relevant parameter controlling lithium diffusion in analyzed perovskites. When the number of vacant sites, n_v, decreases below the percolation threshold, the long-range conductivity decreases drastically.

Conclusion

Structure and ionic mobility has been studied in the crystalline series $Li_{0.5-x}Na_xLa_{0.5}TiO_3$ ($0 \le x \le 0.5$) by means of ND, XRD, NMR, and impedance spectroscopy. As deduced from the Rietveld analysis of ND patterns, Na and La ions occupy A sites, while Li ions are located at the center of unit cell faces of the perovskite. Substitution of Li by Na ions reduces the amount of vacant A sites, and the local mobility of Li ions at room temperature decreases by 2 orders of magnitude along the series. At the same time, long-range dc conductivity values show a sharp decrease at $x = 0.2$, from almost 10^{-3} S/cm to values below 10^{-10} S/cm, which has been ascribed to the percolative blocking of the three-dimensional conduction network. Obtained results confirm the important role played by vacant A sites in Li conductivity of analyzed perovskites.

Acknowledgment. Financial support from CICYT through MAT98 1053-C03 and MAT2001 3713-C03 projects is acknowledged. A.R. acknowledges financial support from Comunidad de Madrid. Authors thank M. T. Fernandez for helpful discussions and ILL for provision of neutron beam time.

CM0204627

(18) Stauffer, D.; Aharony, A. *Introduction to Percolation Theory*; Taylor and Francis: London, 1992.
(19) Wicks, J. D.; Börjesson, L.; Bushnell-Wye, G.; Howells, W. S.; McGreevy, R. L. *Phys. Rev. Lett.* **1995**, *74*, 726.